17β-Estradiol reduces tumor necrosis factor-α-mediated LDL accumulation in the artery wall

Barbara A. Walsh,* Adam E. Mullick,* Rosemary L. Walzem,† and John C. Rutledge[1,*]

Division of Cardiovascular Medicine, Department of Medicine,* Departments of Nutrition and Molecular Biosciences,† University of California, Davis, CA 95616

Abstract **Estrogens have direct effects on the vascular wall that may prevent the development of atherosclerosis. In particular, estrogens, such as 17β-estradiol (estradiol), are known to have potent antioxidant activity. Tumor necrosis factor-α (TNF) is found in human atheroma and produces oxygen-derived free radicals. These oxygen-derived free radicals may modify low density lipoproteins (LDL) and increase LDL binding in the artery wall. We asked: 1) does TNF increase LDL accumulation in the artery wall and 2) can the TNF-mediated increase in LDL accumulation be prevented by the antioxidant activity of estradiol? Carotid arteries from ovariectomized 3-month-old rats were removed and perfused with fluorescently labeled LDL and arterial LDL flux was measured using quantitative fluorescence microscopy. In six arteries, addition of TNF (10 ng/ml) to the perfusate resulted in a 2.3-fold increase in the rate of LDL accumulation (1.50 ± 0.37 ng/min per cm^2 vs. 3.38 ± 0.48 ng/min per cm^2; $P < 0.01$). Estradiol (65 pg/ml) and α-tocopherol (6 mg/L) both attenuated TNF-mediated LDL accumulation ($P < 0.05$), indicating that TNF may exert its effects on LDL accumulation through cellular production of oxygen-derived free radicals. These results support an antioxidant role for estradiol in the protection against LDL accumulation in the artery wall and subsequent progression of atherosclerosis.—**Walsh, B.A ., A. E. Mullick, R. L. Walzem, and J. C. Rutledge. **17β-Estradiol reduces tumor necrosis factor-α-mediated LDL accumulation in the artery wall.** ***J. Lipid Res.*** **1999.** 40: **387–396.**

Supplementary key words lipoprotein flux • sex hormones • carotid arteries • antioxidants • atherosclerosis

Atherosclerosis is characterized, in part, by low density lipoprotein (LDL) accumulation in the artery wall (1). Modification of LDL (for example, oxidation) is known to accelerate the accumulation and degradation of lipoproteins in the artery wall (2), as well as facilitate the uptake of lipoproteins by lipid-filled macrophages (3). Inhibition of lipoprotein modification could prevent LDL accumulation in the artery wall.

Estrogens are known to have powerful protective effects on atherosclerosis (4–6). However, some authors estimate only about 30–50% of estrogen's protective role can be attributed to changes seen in plasma lipid and lipoprotein levels, mainly elevations in HDL cholesterol, HDL_2, and apolipoproteins A-I (7, 8). Recent studies (9, 10) found that hormone replacement therapy reduces LDL uptake and accumulation in the artery wall independent of plasma lipid levels. Therefore, estrogen therapy may act through other mechanisms at the level of the artery wall in order to have such profound atheroprotective effects.

Mounting evidence indicates some estrogens are potent antioxidants. Studies in vitro showed that 17β-estradiol (estradiol), the most abundant estrogen in humans, effectively scavenged 2,2′-azobis (2-amindino-propane) dihydrochloride-generated peroxy radicals while testosterone and progesterone had no effect (11). Also, Rifici and Khachadurian (12) demonstrated that estradiol inhibited both cell-free (copper-catalyzed) and mononuclear cell-mediated oxidation of LDL. Thus, estradiol could potentially prevent LDL modification by antioxidant effects. However, no studies testing the effect of estradiol on LDL modification have been conducted in the artery wall.

Most modification of LDL in the cardiovascular system is thought to occur, not in plasma, but in the vascular wall (1). Tumor necrosis factor-α (TNF) is a cytokine produced by activated macrophages (13) and found in human atheroma (14). In studies performed in cell culture, TNF treatment caused production of superoxide anions in both endothelial cells (15, 16) and smooth muscle cells (17). Maziere, Auclair, and Maziere (18) determined that superoxide anions secreted by cultured monocytes and endothelial cells in response to TNF resulted in oxidation of LDL. TNF, therefore, could be an important mediator of in vivo LDL oxidation through its production of superoxide anions.

The goals of our study were to examine the effect of TNF on LDL flux in the artery wall and to determine whether the antioxidant properties of estradiol could attenuate or prevent LDL accumulation in the artery wall.

Abbreviations: DiI, 1,1-dioctadecyl-3,3,3′,3′-tetramethyl-indocarbocyanine; FITC, fluorescein isothiocyanate; TRITC, tetramethylrhodamine isothiocyanate; X/XO, xanthine/xanthine oxidase.

[1]To whom correspondence should be addressed.

To achieve these goals, the rate of fluorescently labeled LDL accumulation was measured in perfused arteries by quantitative fluorescence microscopy. Our study showed in real time that TNF increased LDL binding and that estradiol and the antioxidant α-tocopherol attenuated LDL accumulation in the artery wall.

MATERIALS AND METHODS

Chemicals and materials

Kreb's-Henseleit buffer consisted of (in mm): NaCl 116, KCl 5, $CaCL_2*H_2O$ 2.4, $MgCl_2$ 1.2, NH_2PO_4 1.2, and glucose 11. 17β-Estradiol (lot #125H1081), α-tocopherol (lot # 85H0988), xanthine (lot #85H7195), xanthine oxidase (lot #105H3896), allopurinol (lot #5H3442), and TRITC-dextran (lot #101H0102) were obtained from Sigma Chemical Co. (St. Louis, MO). TNF from Boehringer Mannheim (Indianapolis, IN; lot #14831200) was used in the perfusion experiments. Modification of LDL was assessed by the Lipo lipoprotein electrophoresis kit from Beckman (Fullerton, CA; lot # M602016). DiI (lot #1651-30) was obtained from Molecular Probes (Eugene, OR).

Fluorescent solutes

LDL was isolated and labeled as described by Pitas et al. (19). Briefly, blood was obtained from fasting human males in Vacutainers containing ethylenediaminetetraacetic acid and centrifuged for 10 min at 2800 rpm at a temperature of 4°C. The plasma was recovered and LDL (d 1.01–1.06 g/ml) and lipoprotein-deficient serum were obtained by sequential density gradient ultracentrifugation. LDL was labeled with the fluorescent hydrocarbon probe 1,1-dioctadecyl-3,3,3′,3-tetramethyl-indocarbocyanine (DiI). The spectral properties of DiI are the following: excitation maximum 540 nm and emission maximum 556 nm. After labeling, the LDL was re-isolated by ultracentrifugation for removal of any contaminants. Prior to arterial perfusion, the labeled LDL (≈1 mg protein/ml) was diluted 1:20 in Kreb's-Henseleit solution (final concentration ≈50 μg LDL-protein/ml) for use in these experiments.

Some arteries were perfused with dextran labeled with fluorescein isothiocyanate (FITC) or tetramethylrhodamine isothiocyanate (TRITC). Dextran was dissolved in H_2O to a concentration of 75 mg/ml and diluted 1:1200 in Kreb's-Henseleit solution (final concentration = 63 μg/ml).

Animal care and ovariectomy surgery

Female Crl:CD® (SD)BR rats (100–150 g) were received from Charles River Laboratories and maintained in a facility approved by the Animal Use Committee at the University of California, Davis. Animals received rat chow and water ad libitum and were kept on a 12:12 h light/dark cycle.

Within a week of their arrival, bilateral ovariectomies were performed on the rats. The animals were anesthetized intraperitoneally (i.p.) with xylazine (10 mg/kg) and ketamine (80 mg/kg). A 1-inch dorsal midline incision through the skin from the second to fifth lumbar vertebrae was made with a scalpel. Two small lateral incisions were made through the muscles in order to reach the fat pads overlying the ovaries. The ovaries were located, a ligature (6-0 silk) was tied at the base of each ovary and the ovary was excised. The dorsal skin incision was sealed with Nexaband™ tissue glue and the animals were given an intramuscular injection of the antibiotic enrofloxine (10 mg/kg) and placed on a heating pad for recovery. Animals were allowed to recover for 1 month before perfusion experiments were performed.

Perfusion experiments

Ovariectomized rats were anesthetized i.p. with 1.5 g urethane/kg body weight and both common carotid arteries were exposed and cannulated as follows. An anterior midline skin incision was made from the mandible to the sternum. The superficial neck muscles were retracted and the carotid arteries were carefully dissected free from surrounding tissue. An incision was made in the proximal artery and a cannula (polyethylene-50 tubing) was inserted and tied into place with 4-0 silk. A second incision was made in the distal portion of the artery, just proximal to the bifurcation of the common carotid artery, and another cannula was inserted and tied into place. Throughout the surgery, the artery was superfused with Kreb's-Henseleit solution. Upon completion of the cannulations, the artery was perfused with Kreb's-Henseleit solution plus 1% bovine serum albumin gassed with 95% compressed air and 5% CO_2 until the start of the experiment. The artery was excised and taken to the experimental rig for the perfusion experiment. During our experiments, the artery is maintained at a constant length from the moment it is cannulated until the time it (via the cannulae) is secured into place in the perfusion chamber. After removal of both carotid arteries, blood was collected from each animal through the right atrium using a 22-gauge needle and a heparinized syringe. Blood was transferred to sterile Vacutainers and centrifuged at 2800 rpm for 10 min. Plasma samples were separated from blood cells and kept at 4°C. These samples were sent to the UC Davis Endocrinology Laboratory for radioimmunoassay analysis of estradiol concentration. Plasma estradiol levels in these ovariectomized rats averaged 20 pg/ml.

Experimental rig

The cannulated artery was placed in a clear fluid-filled superfusate chamber and mounted on a Nikon MM-11 upright microscope stage for viewing. The artery was continuously bathed in a Kreb's-Henseleit solution, which was maintained at 37°C. This was achieved by directing the buffer solution from a reservoir through a heating coil to the superfusate chamber. A thermometer placed in the superfusate chamber monitored the temperature. The temperature of the superfusate solution was adjusted by changing the temperature of the heating coil.

Perfusate flowed through the artery at a physiological flow rate (7 ml/min) and hydrostatic pressure (90 cm H_2O). The perfusate consisted of either *1*) a clear, non-fluorescent solution of Kreb's-Henseleit solution +1% bovine serum albumin or *2*) a fluorescent solution containing the same components as *1*) and fluorescently labeled LDL particles. These perfusate solutions were kept in separate reservoirs and were alternately perfused into the artery via a series of tubing and 2- and 3-way stopcocks (20). Both solutions were maintained at a pH of 7.3–7.4. A 10-cm length of perfusate tubing attached to the proximal cannula was submersed in a 38°C water bath to ensure physiological temperature of the perfusate as it entered the vessel. In addition, all air bubbles were purged from the system.

The portion of the artery in the superfusate chamber to be examined was brought into focus using a Nikon Plan X4 objective (NA 0.1) mounted on the microscope head. Light from a mercury bulb passed through a filter specific for the fluorescent molecules to be excited causing photons to be emitted from the fluorophore. A dual optical path tube transmitted the fluorescence to a Hamamatsu CCD television camera and Nikon P1 photometer and controller. The photons emitted from the fluorophore were captured and quantified by the photometer. Changes in fluorescence intensity were measured by the photometer and input to a chart recorder and computer. A videocassette recorder and high resolution monitor received the output from the television camera (21).

Measurement of LDL accumulation

The photometric measuring window was centered on a segment of the vessel positioned on the microscope stage and fluorescence was captured from this same segment for the duration of the experiment. Also, the same segment of the artery was imaged using the optical system described above. Initially, the artery was perfused with the nonfluorescent solution to determine a baseline level of fluorescence intensity (I_f). Then, the artery was perfused with the buffer solution containing the fluorescently labeled DiI-LDL for 10 min, immediately followed by wash out (10 min) of the fluorescent solution with the clear nonfluorescent solution. This sequence of a 10-min perfusion of the fluorescent solution followed by a 10-min perfusion of the nonfluorescent solution will subsequently be referred to as a "run." When alternating the perfusate flow through the artery from the nonfluorescent solution to the fluorescent solution and vice versa, a momentary drop in pressure, of 10–20 cm H_2O, was observed. This reduction in pressure lasted only a few seconds until the pressure could equilibrate, and at no time during our recordings was the artery under zero pressure or no flow.

Perfusion of the artery with the fluorescent solution resulted in a step increase in the fluorescence intensity (I_{f0}) (**Fig. 1A**). I_{f0} represented the initial fluorescence intensity of the solution filling the artery lumen. During perfusion of fluorescent solution, some fluorescent molecules crossed into the artery wall and/or bound to the endothelium. When the fluorescent solution was washed out by the nonfluorescent solution, there was a rapid drop in fluorescence intensity and I_f approached the previously determined baseline. Fluorescently-labeled LDL molecules remaining in/on the artery wall were designated I_f accumulation (Fig. 1B) and measured in millivolts (mV). We were able to quantify the rate of LDL accumulation in the artery wall by converting the photometric units of mV to the physiological units of ng/min per cm^2 by knowing the following parameters: concentration of DiI-LDL protein in the perfusate solution; I_{fo}, or initial fluorescence of DiI-LDL solution filling the artery lumen in the viewing window; time of DiI-LDL perfusion; and radius and length of the artery in the microscopic viewing window. Utilizing the equation volume = $\pi r^2 l$, combined with the parameters listed above, we determined the volume of DiI-LDL solution viewed by our photometer and from this a μg amount of LDL corresponding to a given mV recording. To illustrate, a typical carotid artery has a radius (r) of 0.05 cm and length (l) of 0.12 cm (a constant due to the physical limitations of the viewing window), giving rise to a volume of 0.000942 ml DiI-LDL solution. With an I_{fo} of 38 mV and concentration of DiI-LDL protein equal to 0.050 mg/ml, we know that the 0.000942 ml volume of LDL solution filling the artery contains 0.0471 μg DiI-LDL. Thus, a photometric reading of 38 mV represents 0.0471 μg DiI-LDL. If after a 10-min perfusion it was observed that this artery accumulated 1 mV of DiI-LDL in the artery wall, this corresponded to an accumulation rate of 3.3 ng/min per cm^2. Rates of accumulation of other fluorescent macromolecules were calculated in the same manner.

To examine the baseline rates of LDL accumulation and the reliability of our measurements over time, six rat carotid arteries

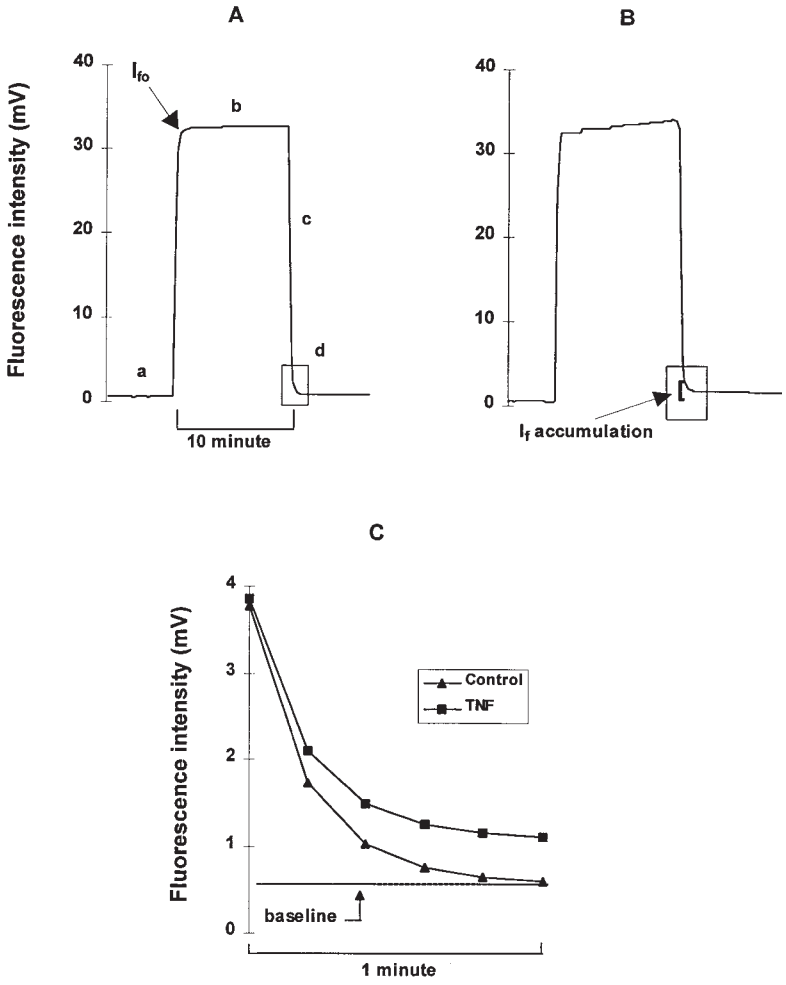

Fig. 1. A: Measurement of fluorescence intensity during perfusion of LDL labeled with DiI. (a): Baseline fluorescence intensity (I_f) obtained during perfusion of the nonfluorescent buffer solution. (b): Perfusion of the buffer solution containing DiI-LDL where I_{fo} represents the fluorescence intensity of the DiI-LDL perfusate initially filling the artery lumen. (c): Washout of the fluorescent LDL solution with nonfluorescent solution. The absence of fluorescence in the buffer solution is the reason for the drop in fluorescence intensity in this short time period (≈5 sec). (d): LDL efflux from the artery wall (see Fig. 1C). B: Effect of treatment with TNF. In the same artery as illustrated in Fig. 1A, TNF (10 ng/ml) was added to the perfusate solutions. Note that the slope of (b) is increased, suggesting increased LDL accumulation in the artery wall. I_f accumulation is the amount of DiI-LDL remaining in/on the artery wall after lumen washout. C: Comparison of LDL efflux from the artery wall after control LDL perfusion and after treatment with TNF ("d" inserts from Figs. 1A and 1B). Note the change in the fluorescence scale. TNF treatment results in increased accumulation and decreased efflux of LDL, indicating increased LDL retention in the artery wall.

were perfused over the course of 3 h and the rate of LDL accumulation was measured (total of 9 measurements of LDL accumulation taken in each artery). Analysis of the data revealed that the rate of LDL accumulation stayed constant over the course of the 3-h period. We found no difference in the rate of LDL accumulation between the first 3 measurements taken in the first hour (1.97 ± 0.59 ng LDL protein/cm^2 per minute) and the last 3 measurements taken in the last hour (2.06 ± 0.43 ng LDL protein/cm^2 per minute). As our experiments described herein did not extend longer than 3 h, we feel confident that our measurements are reliable.

Measurements of the rate of LDL accumulation were performed under control conditions and compared to treatment conditions. Initially, three control runs were performed on every vessel from each group to obtain a control rate of accumulation. Then, depending on the group, an antioxidant and/or oxidant stress treatment was applied to the vessels and accumulation was measured as described above. All treatments were added directly to both the nonfluorescent and fluorescent buffer solutions used to perfuse the arteries.

Minimal photobleaching was observed in our system. We performed control experiments where DiI-LDL, at the same concentration utilized in our experiments, was perfused continuously through polyethylene (PE-50) tubing. Fluorescence intensity was monitored over the course of 90 min. Less then 5% reduction of fluorescence intensity was observed during this time interval. Additionally, utilizing arteries from 3-month-old ovariectomized female rats, we performed control experiments by alternately perfusing arteries with buffer or buffer + DiI-LDL. We found that after 3 h (8 "runs") I_{fo} decreased from an average of 33 mV to 31 mV when the first hour was compared to the last 2 hours. This 6% drop in fluorescence intensity under control conditions indicates minor photobleaching of DiI-LDL over the entire course of the experiments.

Localization of DiI-labeled LDL in the artery wall

To determine whether LDL accumulated on the artery endothelial surface and/or in the artery wall, we imaged LDL localization after treatment with TNF. The carotid artery segment was fixed with O.C.T. (Tissue-Tec), placed on dry ice and stored at −80°C. Frozen cryosections of the artery (4 μm thick) were examined with a Zeiss Axioskop MC80 equipped with a Dage DC 330 3CCD color camera interfaced with the Scion LG-3/PCI board and PowerPC 7200 MacIntosh. A 20× objective lens was used to image the sections. The same field was captured under fluorescent light with an excitation filter of 530–580 nm and an emission filter of 650 nm (rhodamine filter) and under phase contrast microscopy. The captured images were stored as 24-bit NIH files. Using Adobe Photoshop, the fluorescent image was layered over the phase-contrast image so that the location of the fluorescence could be determined. The images were printed on Codonics NP-1600 dye sublimation printer.

Analysis of LDL particle diameter distributions

Particle diameter distributions were measured by dynamic laser light scattering as described previously (22) with the following modifications. Sample LDL were assumed to be non-spherical, transparent particles of d 1.04 g/ml with a refractive index of 1.47. Values were expressed as particle volume distributions (23). Particle diameter distributions were determined for prepared LDL recovered from the perfusate of isolated vessels.

Statistical analysis

For each artery, the rate of LDL accumulation was measured for each run. A control rate of LDL accumulation was determined by averaging the rate of accumulation for the three runs of the experiment performed under control conditions. Then, treatments (TNF, estradiol, xanthine/xanthine oxidase, or α-tocopherol) were added to the perfusate solutions and the rate of LDL accumulation was determined for each run. The mean and standard error of the mean were determined for each treatment group.

All statistical analyses utilized SigmaStat 1.0 software by Jandel Scientific Software. The rate of accumulation change due to a single treatment within the same group was analyzed by paired *t* test. Effects of multiple treatments within the same group of vessels and differences in the % change across treatment groups were analyzed by one-way repeated measures ANOVA and one-way ANOVA, respectively. Student-Newman-Keuls post hoc test was used to analyze for significant effects. Tests of significance were applied at the 5% level.

RESULTS

TNF increases LDL accumulation in the artery wall

Preliminary experiments were performed with TNF at a range of concentrations (fg/ml–ng/ml). The experiments described below were performed at a concentra-

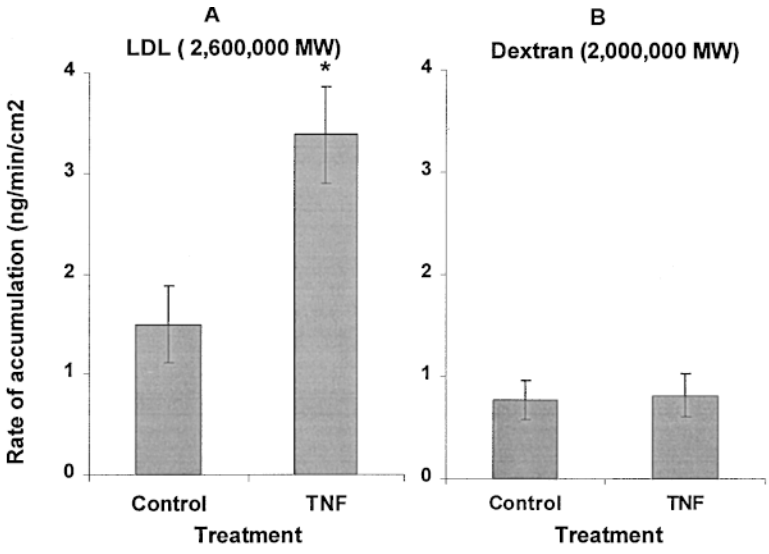

Fig. 2. TNF effects on rates of LDL (A) and dextran (B) accumulation. Mean values for the rates of accumulation of LDL and dextran before (control) and after (TNF) 10 ng/ml TNF treatment. Compared with control values, TNF significantly increased rate of LDL accumulation (* = $P < 0.05$) with no effect on dextran 2,000,000 MW accumulation rate.

tion of 10 ng/ml TNF because of the predictable increase in LDL accumulation noted with this concentration (the concentration of TNF determined in atherosclerotic arterial wall tissue (2–13 ng/ml) (24) was about this value) and for comparison with previous cell culture and microvessel experiments by others using this concentration (15, 18). In six arteries, the rate of LDL accumulation was determined at control (1.50 ± 0.37 ng/min per cm^2). Then, TNF was added to both the fluorescent and nonfluorescent solutions at a concentration of 10 ng/ml. The addition of TNF caused a 2.3-fold increase in the rate of LDL accumulation compared to control values (3.38 ± 0.48 ng/min per cm^2; $P < 0.01$; Figs. 1B, 1C, and **Fig. 2A**). Increased LDL accumulation rates were detected after only 10 min of TNF treatment and remained elevated throughout the entire time of TNF exposure (1.5 h). Serial sections of a carotid artery (**Fig. 3**) showed that LDL accumulated in the subendothelial and medial portions of the artery after exposure to TNF.

We examined LDL particles using dynamic laser light scattering to detect differences in perfused LDL after treatment of the artery with TNF. Fluorescently labeled LDL had a monomodal polydisperse particle size distribution with a mean particle diameter of 19.9 nm in a control artery perfused for 2 h, not treated with TNF (**Fig. 4**, panel A). In another artery, LDL was perfused for 1 h at control followed by addition of TNF. One hour after addition of TNF to the perfusate, a sample of the perfusate was taken. In the TNF-treated artery LDL exhibited a trimodal particle population distribution indicative of particle aggregation (Fig. 4, panel B). The smallest particle population had a mean diameter of 43.8 nm and represented 83% of the material analyzed. These results suggest that LDL dimerize prior to forming larger aggregates.

Effect of TNF on reference molecule accumulation in the artery wall

TNF has been shown both in in vivo studies (25) and cell culture studies (26) to increase permeability. To determine whether TNF increased permeability and caused an increase in macromolecule accumulation, we measured the rate of accumulation of a non-lipid, water-soluble reference molecule (dextran) in a range of sizes (mol wt 4,000, 76,000, and 2,000,000) under the same conditions as described above. Arterial treatment with TNF resulted in a slight but significant increase in 4,000 MW TRITC-dextran (1.4-fold, n = 2) and 76,000 MW TRITC-dextran (1.2-fold, n = 4) rate of accumulation ($P < 0.01$). Alternatively, TNF treatment had no effect on 2,000,000 MW FITC-dextran rate of accumulation (n = 4; see Fig. 2B). These data suggest that TNF increased arterial permeability to smaller molecules but did not affect permeability to larger macromolecules. The greater relative accumulation of the much larger LDL particle (2,600,000 MW) than the smaller dextran molecules indicates other mechanisms of LDL accumulation in the artery wall. Increased binding of LDL to the artery wall, rather than a change in permeability, could account for this effect.

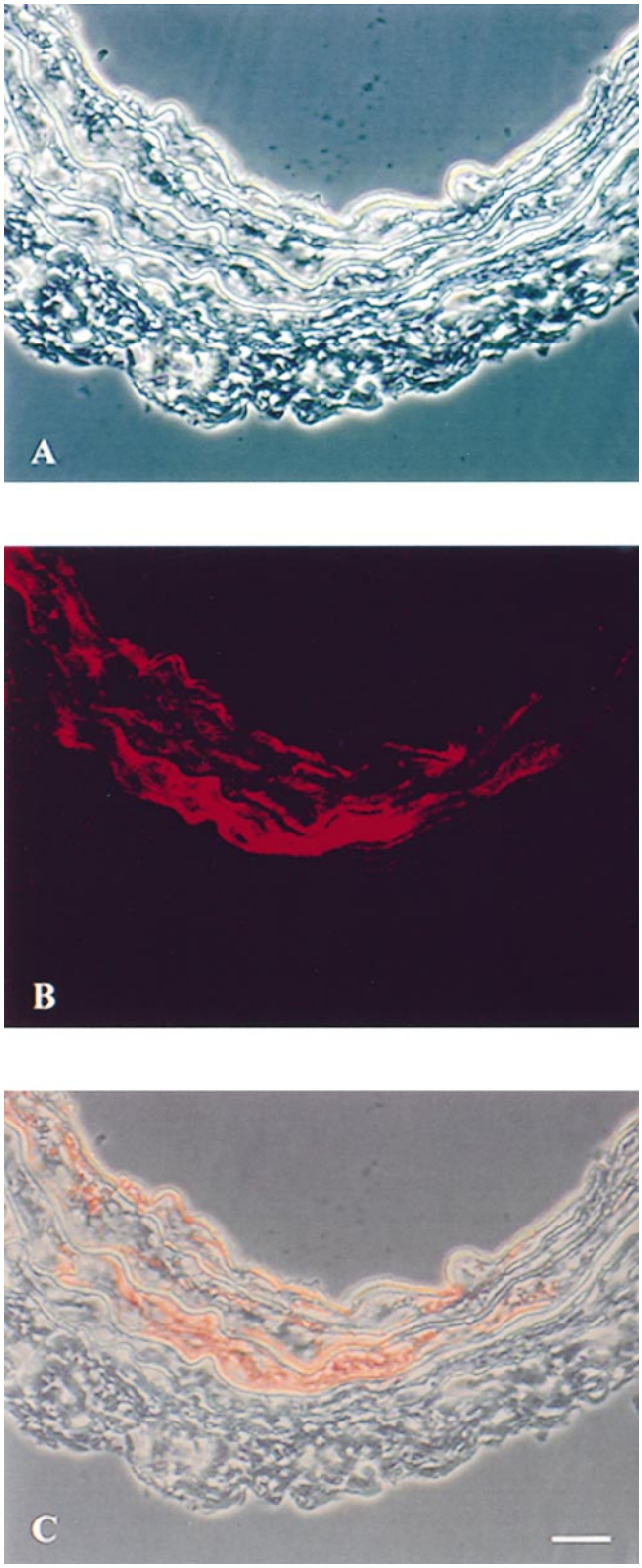

Fig. 3. Localization of LDL in the artery wall after treatment with TNF. (A) Phase contrast microscopy showing a coronal section of the artery wall. (B) Fluorescence microscopy of the same section of artery. Subendothelial circumferential fluorescence (DiI-LDL) was detected in the artery wall. (C) The fluorescent image was layered over the phase-contrast image so that the location of the fluorescence could be determined. The dimension bar is 20 μm long. DiI-LDL was localized as subendothelial/medial LDL accumulation. No LDL was found in the adventitial tissue.

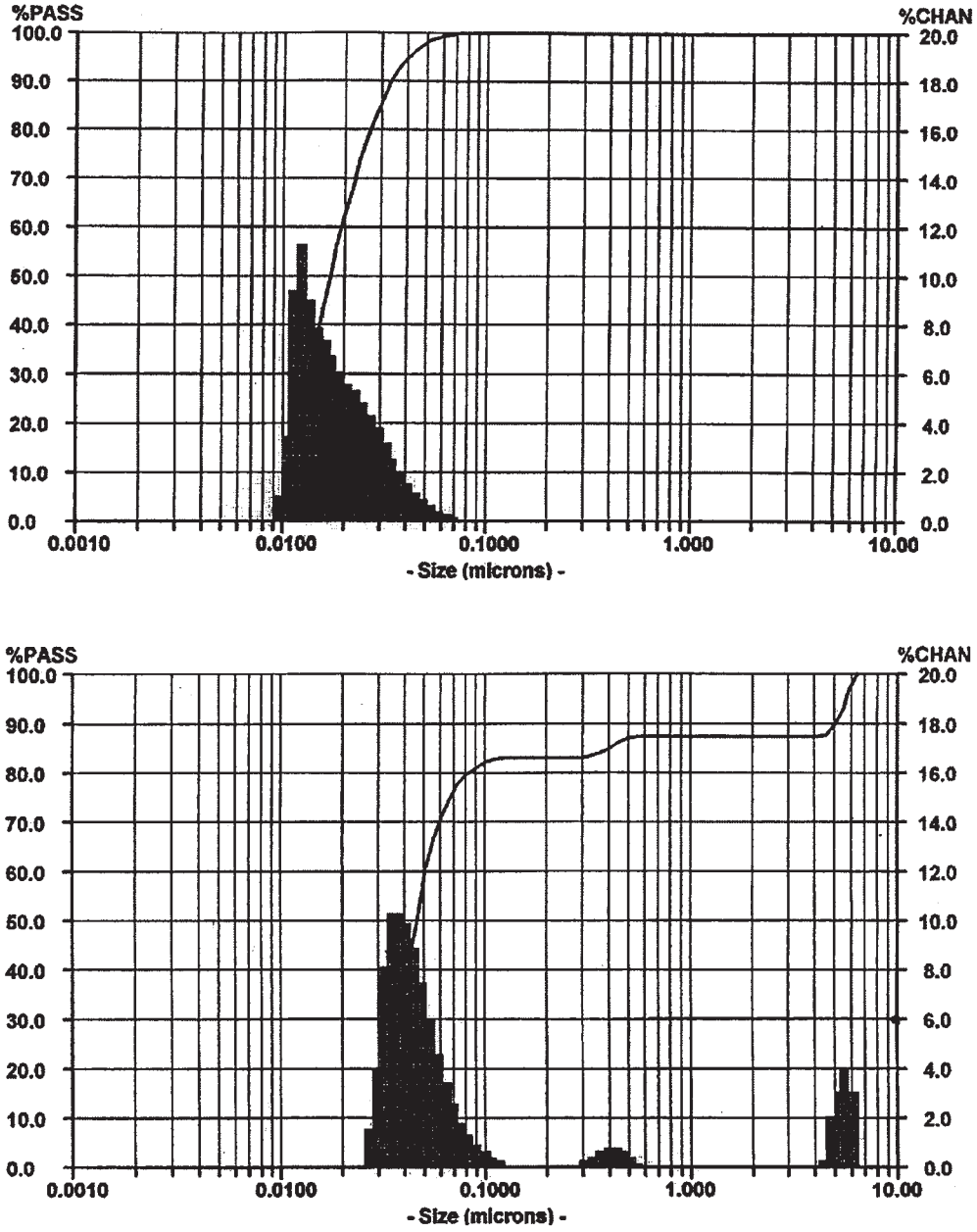

Fig. 4. Particle size distributions determined by dynamic laser light scattering as described in Methods for LDL recovered from isolated perfused blood vessels after 2 h of perfusion. Upper panel is perfusate sample taken from two vessels during control perfusions; lower panel is perfusate taken from two other vessels after 1 h of TNF treatment. LDL 39 were assumed to be non-spherical, transparent particles with a refractive index of 1.47 and d 1.04 g/ml; particle diameter distribution in microns is presented as particle volume distribution. Histogram bars represent the percentage of total LDL volume present as particles of the specified diameter, % in channel (CHAN). Line graph represents the cumulative percentage of particles with diameters smaller than the specified channel edge, % PASS.

Superoxide generation increases LDL accumulation in the artery wall

To examine whether LDL accumulation was altered by the superoxide anion generation, we exposed DiI-LDL to a well-known system for superoxide anion generation, xanthine-xanthine oxidase. In five vessels, the rate of LDL accumulation was determined before and after addition of xanthine (0.4 mg/ml) and xanthine oxidase (0.2 mg/ml) to the fluorescent solution. Enzymatic production of superoxide in the presence of LDL resulted in a 3-fold increase in LDL accumulation over control (5.11 ± 46 ng/min per cm^2 versus 15.6 ± 2.6 ng/min per cm^2; $P = 0.02$). Agarose gel electrophoresis of X/XO-exposed LDL showed an altered migration pattern, indicative of LDL modification (data not shown). Addition of either xanthine or xanthine oxidase alone had no effect on LDL accumulation.

Effect of estradiol on TNF-mediated LDL accumulation

In eight vessels the rate of DiI-LDL accumulation was determined at control, after addition of a physiological concentration (27) of estradiol (65 pg/ml) to the perfusate solutions and after addition of TNF (10 ng/ml) in the presence of estradiol. As compared to control (3.22 ± 0.33 ng/min per cm^2), no change in the rate of LDL accumulation was seen with estradiol treatment (3.58 ± 0.34 ng/min per cm^2). TNF treatment, however, resulted in an increase in rate of LDL accumulation to 4.34 ± 0.33 ng/min per cm^2. This small, but significant ($P < 0.01$), increase was 1.3- and 1.2-fold greater than the control and estradiol-treated rates of accumulation, respectively. In comparison, TNF alone increased the rate of LDL accumulation 2.3-fold over control values.

Estradiol attenuates xanthine/xanthine oxidase-induced increase in LDL accumulation

We then tested the effects of estradiol on LDL accumulation in the presence of superoxide anions. In seven vessels, the rate of LDL accumulation was determined at control and in the presence of 65 pg/ml estradiol. Consistent with earlier findings, there was no effect on rate of LDL accumulation with the addition of estradiol (4.3 ± 0.60 ng/min per cm^2 versus 4.95 ± 0.98 ng/min per cm^2). Addition of xanthine (0.4 mg/ml) and xanthine oxidase (0.2 mg/ml) to these estrogen-treated vessels resulted in a significant 1.8-fold increase (8.95 ± 1.55 ng/min per cm^2; $P < 0.01$) in rate of LDL accumulation. This 95% increase in LDL accumulation was significantly less than the 217% increase seen when vessels were perfused with xanthine/xanthine oxidase without estradiol pretreatment ($P < 0.05$).

α-Tocopherol attenuates TNF-induced LDL accumulation

Next, we examined the effects of a potent lipid-soluble antioxidant, α-tocopherol, on TNF-mediated increases in LDL accumulation. A physiological dose (28) of α-tocopherol (6 mg/L) was added to the perfusate and the rate of LDL accumulation decreased slightly from 3.25 ± 0.53 ng/min per cm^2 to 2.73 ± 0.71 ng/min per cm^2. After pretreatment of the vessels with α-tocopherol, addition of TNF (10 ng/ml) resulted in a small increase in LDL accumulation rate (3.53 ± 1.02 ng/min per cm^2). There was no significant difference among the three treatments.

Modulation of TNF-induced LDL accumulation by superoxide dismutase

Experiments were performed to assess the effects of the superoxide scavenger, superoxide dismutase (SOD), on the TNF-induced LDL oxidation and vascular uptake. A dose–response evaluation indicated that SOD in concentrations of 2.5 mg/L or greater resulted in increased LDL accumulation rates approximately 30–50% over that measured under control conditions. SOD (0.5–1 mg/L) applied to the perfusate (n = 3 vessels) completely blocked the effect of TNF on LDL accumulation rate (4.82 ± 1.09 ng/min per cm^2; 4.80 ± 0.59 ng/min per cm^2; and 4.69 ± 0.64 ng/min per cm^2 for control, SOD, and SOD + 10 ng/ml TNF, respectively). Catalase, in conjunction with SOD, was not required for the protective effect. In fact, addition of catalase alone (1200 U/ml) or in the presence of SOD resulted in an increased baseline rate of LDL accumulation, possibly due to the presence of iron in the solute.

Comparison across treatment groups

In order to examine treatment effects on TNF-induced increases in the rate of LDL accumulation, we analyzed the percent change in rate of LDL accumulation (**Fig. 5**). We compared the % change in the rate of LDL accumulation due to TNF treatment among these three groups of vessels: *1*) control; *2*) estradiol-pretreatment, and *3*) α-tocopherol-pretreatment. ANOVA of the percent change among the groups showed that the change in the control group after treatment with TNF (228 ± 116 %) was significantly greater than the estradiol-pretreatment and α-tocopherol-pretreatment groups (26 ± 10% and 25 ± 15%, respectively; $P < 0.05$). Estradiol-pretreatment and α-tocopherol-pretreatment groups were not different from each other. Thus, both α-tocopherol and estradiol significantly reduced LDL accumulation mediated by TNF.

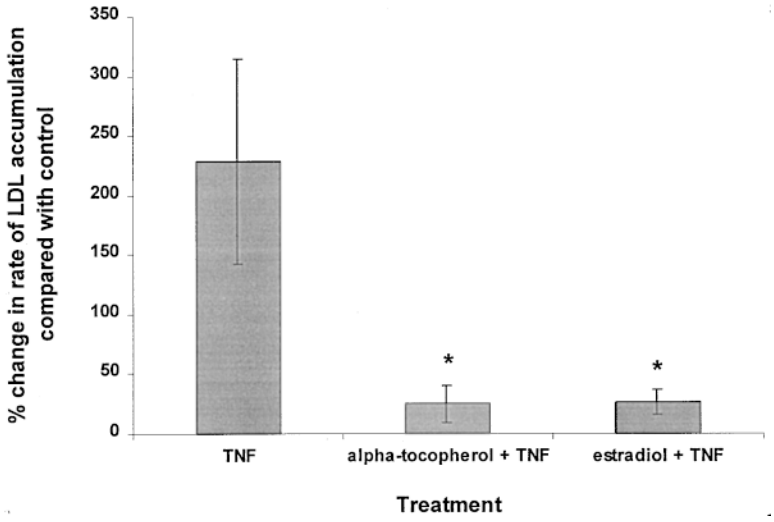

Fig. 5. Percent change in the rate of LDL accumulation with TNF, α-tocopherol + TNF and estradiol + TNF compared with control rates of LDL accumulation. Both α-tocopherol and estradiol significantly attenuated the expected TNF increase in the rate of LDL accumulation (* = $P < 0.05$).

DISCUSSION

Our studies demonstrated a mechanism of estrogen-mediated protection against LDL accumulation at the level of the artery wall. TNF increased LDL binding in the artery wall and resulted in increased LDL accumulation. Although TNF increased permeability, the major TNF-mediated effect appeared to be specific to the interaction and binding of LDL with the artery wall. Addition of estradiol and α-tocopherol, both antioxidants, attenuated the TNF effect. These studies indicate a potential mechanism by which this ubiquitous female sex hormone could protect against the development of atherosclerosis.

Our experimental preparation allows us to make serial real time measurements of LDL accumulation in individually perfused arteries under carefully controlled conditions. Many previous studies have not controlled for regional differences in physical stresses applied to the artery wall or composition of the blood (for example, lipoproteins). Previous studies from our lab (29) and others (30) indicate macromolecule flux in the artery wall is sensitive to physical parameters (for example, hydrostatic pressure). In our preparation, perfusate flow and hydrostatic pressure, as well as the perfusate and superfusate composition, are exactly known and can be manipulated. Thus, the effects of estradiol on the artery wall can be studied without the complicating hemodynamic variables associated with regional circulations. Although the rat carotid artery is not a model of atherosclerosis, by utilizing this experimental preparation, we are able to examine lipoprotein interactions with the artery wall, uncomplicated by compounding factors such as the presence and/or progression of vascular disease.

We chose the cytokine TNF for use in these experiments based on the large body of evidence supporting TNF as a potent bioactive substance acting on the vascular wall and present in atheroma. We were specifically interested in TNF because previous reports indicated that TNF caused immediate production of superoxide anions (15–17) and these oxygen radicals resulted in oxidation of LDL (18). Both endothelial cells and smooth muscle cells in the artery wall contain TNF receptors and have the potential to respond to this cytokine (31). Although TNF has a number of cellular effects including expression of adhesion molecules, phenotypic and qualitative alteration of smooth muscle cells, apoptotic cell death, inflammation, and angiogenesis (32), the short exposure time of the vessel to TNF and absence of an immune response suggest that these effects did not play a role in our experimental findings.

The early effect that we observed with TNF provided a potential mechanism to modify LDL in vivo and study the effect of female sex hormones on LDL modification and flux in the artery wall. Although the specific mechanism through which TNF acts to augment superoxide anion production has not been elucidated, many mechanisms have been implicated. Beyaert and Fiers (33) suggest that mitochondrial reactive oxygen formation may occur directly through a TNF/TNF receptor binding effect or, indirectly, involving second messengers such as G-protein-activated phospholipase C, inositol triphosphate, and calcium.

It is possible that LDL was modified in these studies after arterial treatment with TNF. LDL aggregation occurs in vitro in response to a variety of chemical, enzymatic, and physical processes (34) and is thought to contribute to LDL atherogenicity (35). Meyer et al. (36) used neutron solution scattering to show that Cu^{2+}-induced LDL oxidation resulted in a time- and temperature-dependent formation of LDL dimers, trimers, and higher oligomers. The results in Fig. 4 show that perfusion of LDL through a vessel exposed to TNF also causes LDL aggregation, with the majority of LDL forming dimers or trimers within a 3-h period.

We analyzed TNF-treated arteries to discern whether accumulated LDL was localized to the endothelial surface of the artery wall or in the artery wall. As mentioned earlier, DiI-LDL was found in the subendothelial space and media. This finding is consistent with the scanning electron microscopic study of Wasano and Yamamoto (37). They described the internal elastic lamina of the rat aorta and femoral artery as containing various fenestrations from 1–5 μm in size and tunnel-like compartments free of elastic tissue that extended helically into the medial wall of these arteries. Thus, pathways are present for the LDL to pass into the medial layers of the artery wall. Also, rather than accumulating on the endothelium, LDL accumulated in the artery wall. This finding is consistent with LDL modification in the artery wall rather than in the lumen of the artery.

Most cell culture (26) and microvascular (25) experiments describe an increase in endothelial permeability with TNF exposure. Our experiments are consistent with the majority in that TNF caused an increase in estimated permeability to smaller molecules, as seen with the slight increase in dextran 4,000 and 76,000 MW accumulation. Interestingly, we saw no difference in estimated permeability to the much larger 2,000,000 MW dextran molecule. Scanning electron microscopy of TNF-treated arteries showed no morphological differences when compared to control (data not shown). The greater relative accumulation of LDL than a similar-sized reference molecule, in conjunction with the lack of luminal morphological alterations, indicates that mechanisms other than changes in permeability are operative in our perfused arteries.

We saw attenuation of the TNF-induced increase in LDL accumulation with perfusion of the vessels with physiological levels of α-tocopherol. This was presumably due to α-tocopherol acting as a chain-breaking antioxidant, and protecting LDL from oxidation by oxygen-derived free radicals (38). Other researchers have reported that antioxidants, including α-tocopherol, decrease permeability in the injured vascular endothelium through their antioxidant and/or membrane stabilization properties (39). The slight decrease in LDL accumulation rate compared to control observed when the vessels were treated with α-tocopherol was an interesting finding in this study. This may be due to a lowering of the basal permeability levels through stabilization of the endothelial barrier. This ob-

servation suggests another means by which α-tocopherol could protect against atherosclerosis.

These data indicate that one mechanism by which estradiol mediates its effects in the artery wall is through its antioxidant activity. However, other observations also support the hypothesis that estradiol acts as an antioxidant to decrease LDL binding to the artery wall. Estradiol reduces LDL accumulation from xanthine/xanthine oxidase generation of superoxide. The estradiol effect is immediate, implying a non-genomic effect, and within the correct time frame for generation of oxygen radicals. Further, estradiol has a biochemical structure similar to α-tocopherol, a lipophilic antioxidant. Finally, estradiol has been shown to act as an antioxidant in a number of biological and biochemical systems (40, 41). These studies indicate that estradiol reduces the binding and retention of LDL in the artery wall in response to a TNF-induced oxidant stress.

The studies presented in this paper examine the acute administration of TNF and estradiol in the artery wall. We performed these studies in order to understand primary mechanisms whereby estradiol affects vascular wall function. These acute studies will form the basis for further studies that examine chronic effects of sex hormones and potential secondary and tertiary effects on the artery wall.

In conclusion, TNF, and perhaps other molecules that generate reactive oxygen species, increase LDL accumulation and retention in the artery wall, cardinal features associated with the development and progression of atherosclerosis. Our studies demonstrate that estradiol protects against the potentially harmful effects of this inflammatory mediator known to be an important biologic intermediary in atherosclerosis. Thus, our studies suggest a possible mechanistic basis by which female sex hormones exert their beneficial effect on prevention of atherosclerosis.

The authors thank Kristine Lewis and Jason Keledjian for their technical assistance and Charles O'Neil, Ph.D. and Paul Davis, Ph.D. for continued advice. This research was supported by a grant from the National Institutes of Health Heart, Lung, and Blood Institute (RO1 HL 55667).

Manuscript received 23 March 1998 and in revised form 20 August 1998.

REFERENCES

1. Steinberg, D., S. Parthasarathy, T. E. Carew, J. C. Khoo, and J. L. Witzum. 1989. Beyond cholesterol. Modifications of low-density lipoprotein that increase its atherogenicity. *N. Engl. J. Med.* **320:** 915–924.
2. Juul, K., L. B. Nielson, K. Munkholm, S. Stenders, and B. G. Nordestgaard. 1996. Oxidation of plasma low-density lipoprotein accelerates its accumulation and degradation in the arterial wall in vivo. *Circulation*. **94:** 1698–1704.
3. Goldstein, J. L., Y. K. Ho, S. K. Basu, and M. S. Brown. 1979. Binding site on macrophages that mediates the uptake and degradation of acetylated low density lipoprotein, producing massive cholesterol deposition. *Proc. Natl. Acad. Sci. USA.* **76:** 333–337.
4. Godsland, I. F., V. Wynn, D. Crook, and N. E. Miller. 1987. Sex, plasma lipoproteins, and atherosclerosis: prevailing assumptions and outstanding questions. *Am. Heart J.* **114:** 1467–1503.
5. Williams, J. K., M. R. Adams, and H. S. Klopfenstein. 1990. Estrogen modulates responses of atherosclerotic coronary arteries. *Circulation*. **81:** 1680–1687.
6. Williams, J. K., M. S. Anthony, E. K. Honore, D. M. Herrington, T. M. Morgan, T. C. Register, and T. B. Clarkson. 1995. Regression of atherosclerosis in female monkeys. *Arterioscler. Thromb. Vasc. Biol.* **15:** 827–836.
7. Bush, T. L., and E. Barrett-Conner. 1985. Noncontraceptive estrogen use and cardiovascular disease. *Epidemiol. Rev.* **7:** 89–104.
8. Deeley, R. G., S. P. Tam, and T. K. Archer. 1985. The effects of estrogen on apolipoprotein synthesis. *Can. J. Biochem. Cell Biol.* **63:** 882–889.
9. Wagner, J. D., T. B. Clarkson, R. W. St. Clair, D. C. Schwenke, C. A. Shively, and M. R. Adams. 1991. Estrogen and progesterone replacement therapy reduces LDL accumulation in the coronary arteries of surgically postmenopausal cynomolgus monkeys. *J. Clin. Invest.* **88:** 1995–2002.
10. Wagner, J. D., R. W. St. Clair, D. C. Schwenke, C. A. Shively, M. R. Adams, and T. B. Clarkson. 1992. Regional differences in arterial low-density lipoprotein metabolism in surgically postmenopausal cynomolgous monkeys: effects of estrogen and progesterone therapy. *Arterioscler. Thromb.* **12:** 717–726.
11. Mooradian, A. D. 1993. Antioxidant properties of steroids. *J. Steroid Biochem. Mol. Biol.* **45:** 509–511.
12. Rifici, V. A., and A. K. Khachadurian. 1992. The inhibition of low-density lipoprotein oxidation by 17β-estradiol. *Metabolism.* **41:** 1110–1114.
13. Mannel, D. N., R. N. Moore, and S. E. Mergenhagen. 1980. Macrophages as a source of tumoricidal activity (tumor-necrotizing factor). *Infect. Immun.* **30:** 523–530.
14. Barath, P., M. C. Fishbein, J. Cao, J. Berenson, R. H. Helfant, and J. S. Forrester. 1990. Detection and localization of tumor necrosis factor in human atheroma. *Am. J. Cardiol.* **65:** 297–302.
15. Murphy, H. S., J. A. Shayman, G. O. Till, M. Mahrougui, C. B. Owens, U. S. Ryan, and P. A. Ward. 1992. Superoxide responses of endothelial cells to C5a and TNF-alpha: divergent signal transduction pathways. *Am. J. Physiol.* **263:** L51–59.
16. Weber, C. A. Pietsch, W. Erl, M. Strobel, H. W. Loms Ziegler-Heitbrock, and P. C. Weber. 1994. Antioxidants inhibit monocyte adhesion by suppressing nuclear factor-κβ mobilization and induction of vascular cell adhesion molecule-1 in endothelial cells stimulated to generate radicals. *Arterioscler. Thromb.* **14:** 1665–1673.
17. Mensink, A., L. H. J. de Haan, C. M. M. Lakemond, C. A. Koelman, and J. H. Koeman. 1995. Inhibition of gap junctional intercellular communication between primary smooth muscle cells by tumor necrosis factor alpha. *Carcinogenesis.* **16:** 2063–2067.
18. Maziere, C., M. Auclair, and J. C. Maziere. 1994. Tumor necrosis factor enhances low density lipoprotein modification by monocytes and endothelial cells. *FEBS Lett.* **338:** 43–46.
19. Pitas, R. E., T. L. Innerarity, J. N. Weinstein, and R. W. Mahley. 1981. Acetoacetylated lipoproteins used to distinguish fibroblasts from macrophages in vitro by fluorescence microscopy. *Arteriosclerosis.* **1:** 177–185.
20. Roberts, K. A., A. A. Rezai, K. E. Pinkerton, and J. C. Rutledge. 1996. Effect of environmental tobacco smoke on LDL accumulation in the artery wall. *Circulation*. **94:** 2248–2253.
21. Rutledge, J. C., M. M. Woo, A. A. Rezai, L. K. Curtiss, and I. J. Goldberg. 1997. Lipoprotein lipase increases lipoprotein binding to the artery wall and increases endothelial layer permeability by formation of lipolysis products. *Circ. Res.* **80:** 819–828.
22. Walzem, R. L., P. D. Davis, and R. J. Hansen. 1994. Overfeeding increases very low density lipoprotein diameter and causes the appearance of a unique lipoprotein particle in association with failed yolk deposition. *J. Lipid Res.* **35:** 1354–1366.
23. Walzem, R. L. 1996. Lipoproteins and the laying hen: form follows function. *Poult. Avian Biol. Rev.* **7:** 31–64.
24. Rus, H. G., F. Niculescu, and R. Vlaicu. 1991. Tumor necrosis factor-alpha in human arterial wall with atherosclerosis. *Atherosclerosis.* **89:** 247–254.
25. Matsuki, T., J. M. Beach, R. L. Klindt, and B. R. Duling. 1993. Modification of vascular reactivity by alteration of intimal permeability: effect of TNF-alpha. *Am. J. Physiol.* **264:** H1847–1853.
26. Wheatley, E. M., P. J. McKeown-Longo, P. A. Vincent, and T. M. Saba. 1993. Incorporation of fibronectin into matrix decreases TNF-induced increase in endothelial monolayer permeability. *Am. J. Physiol.* **265:** L148–157.
27. Smith, M. S., M. E. Freeman, and J. D. Neill. 1975. The control of progesterone secretion during the estrous cycle and early pseudopregnancy in the rat: prolactin, gonadotropin and steroid

levels associated with rescue of the corpus luteum of pseudopregnancy. *Endocrinology.* **96:** 219–226.
28. Ziouzenkova, O., B. M. Winklhofer-Roob, H. Puhl, J. M. Roob, and H. Esterbaur. 1996. Lack of correlation between the α-tocopherol content of plasma and LDL, but high correlation for δ-tocopherol and carotenoids. *J. Lipid Res.* **37:** 1936–1946.
29. Rutledge, J. C. 1992. Temperature and hydrostatic pressure-dependent pathways of low-density lipoprotein transport across a microvascular barrier. *Am. J. Physiol.* **262:** H234–245.
30. Nielson, L. B., S. Stenders, K. Kjeldsen, and B. G. Nordestgaard. 1994. Effect of angiotensin II and enalapril on transfer of low-density lipoprotein into aortic intima in rabbits. *Circ. Res.* **75:** 63–69.
31. Beutler, B., and A. Cerami. 1988. Tumor necrosis, cachexia, shock and inflammation: A common mediator. *Annu. Rev. Biochem.* **57:** 505–518.
32. Libby, P., and S. K. Clinton. 1992. Cytokines as mediators of vascular pathology. *Nouv. Rev. Fr. Hematol.* **34:** S47–53.
33. Beyaert, R., and W. Fiers. 1994. Molecular mechanisms of tumor necrosis factor-induced cytotoxicity. What we understand and what we do not. *FEBS Lett.* **340:** 9–16.
34. Pentikainen, M. O., E. M. Lehtonen, and P. T. Kovanen. 1996. Aggregation and fusion of modified low density lipoprotein. *J. Lipid Res.* **37:** 2638–2649.
35. Khoo, J. C., E. Miller, P. McLoughlin, and D. Steinberg. 1988. Enhanced macrophage uptake of low density lipoprotein after self-aggregation. *Arteriosclerosis.* **8:** 348–358.
36. Meyer, D. F., M. O. Mayans, P. H. E. Groot, K. E. Suckling, K. R. Bruckdorfer, and S. J. Perkins. 1995. Time-course studies by neutron solution scattering and biochemical assays of the aggregation of human low-density lipoprotein during Cu^{2+}-induced oxidation. *Biochem. J.* **310:** 417–425.
37. Wasano, K., and T. Yamamoto. 1983. Tridimensional architecture of elastic tissue in the rat aorta and femoral artery—a scanning electron microscope study. *J. Electron Microsc.* **32:** 33–44.
38. Frei, B., and J. M. Gaziano. 1993. Content of antioxidants, preformed lipid hydroperoxides, and cholesterol as predictors of the susceptibility of human LDL to metal ion-dependent and independent oxidation. *J. Lipid Res.* **34:** 2135–2145.
39. Urano, S., Y. Inomori, T. Sugawara, Y. Kato, M. Kitahara, Y. Hasegawa, M. Matsuo, and K. Mukai. 1992. Vitamin E: inhibition of retinol-induced hemolysis and membrane-stabilizing behavior. *J. Biol. Chem.* **267:** 18365–18370.
40. Subbiah, M. T., B. Kessel, M. Agrawal, R. Rajan, W. Abplanalp, and Z. Rymaszewski. 1993. Antioxidant potential of specific estrogens on lipid peroxidation. *J. Clin. Endocrinol. Metab.* **77:** 1095–1097.
41. Keaney, J. F. J., G. T. Schwaery, A. Xu, R. J. Nicolosi, J. Loscalzo, T. L. Foxall, and J. A. Vita. 1994. 17-Beta estradiol preserves endothelial vasodilator function and limits low-density lipoprotein oxidation in hypercholesterolemic swine. *Circulation.* **89:** 2251–2259.